Received: 4 November 2019 | Revised: 30 October 2020 | Accepted: 17 November 2020

IET Microwaves, Antennas & Propagation

DOI: 10.1049/mia2.12058

The Institution of Engineering and Technology WILEY

ORIGINAL RESEARCH PAPER

Compact 0.5–18 GHz double-ridged guide horn antenna

Bennie Jacobs[1,2] | **Johann W. Odendaal**[1] | **Johan Joubert**[1]

[1]Centre for Electromagnetism, University of Pretoria, Pretoria, South-Africa

[2]Saab Grintek Defence, Centurion, South-Africa

Correspondence

Bennie Jacobs Centre for Electromagnetism, University of Pretoria, Pretoria, South-Africa.
Email: bennie.jacobs@za.saabgroup.com

Abstract

Broadband double-ridged guide horn (DRGH) antennas are extensively used in antenna measurement and electromagnetic compatibility and interference testing, especially the 1–18 GHz DRGH antenna which is widely accepted as a standard for this band. Certain deficiencies in the radiation patterns have been identified and corrected by several authors, but the use was still limited to the 1–18 GHz frequency band. The incorporation of absorber materials and lenses has resulted in horn antennas with wider bandwidths; however, this complicates the manufacturing process and restricts these designs to lower power applications. Simulated and measured results for a new 0.5–18 GHz (36:1) DRGH antenna are presented here. The wider bandwidth is made possible by a new cavity design and optimising the design of the other antenna sections to allow wideband operation without using a lens or absorber. The new design has double the bandwidth ratio and is very compact, with an aperture size of 26.4 cm × 15.2 cm; the aperture sides are less than 12% larger than the sides of the aperture of the conventional 1–18 GHz DRGH antenna (24.2 cm × 13.6 cm).

1 | INTRODUCTION

Broadband double-ridged guide horn (DRGH) antennas are extensively used for various applications namely antenna measurement (both as reference and source antennas), electromagnetic compatibility and interference (EMC/I) testing, communication systems, satellite tracking systems, feeds for reflectors and electronic warfare (EW). Features that have contributed to this wide-spread use are high gain, wide bandwidth, high power handling, good pattern behaviour, easy excitation and comparatively simple construction.

Some of the first DRGH antenna designs were presented in [1,2]. Most of the early work focused on extending the bandwidth ratio from 3:1 to typically around 11:1. The only available tools to perform design and analysis at that time were experimentation and semi-analytical methods such as radio frequency (RF) network theory [3,4]. Further development resulted in a 1–12 GHz design with a usable impedance bandwidth ratio approaching 18:1 [5–7]. Derivatives of this 1–18 GHz DRGH antenna design are in widespread use, for example, for EMC/I testing according to MIL-STD-461. Significant pattern deterioration of these antennas above 12 GHz was reported in [8–10], which limits their application. Subsequent research on DRGH antenna design resolved the pattern deterioration problem [11–13]. Tolerance and sensitivity studies were also performed [14,15] , the effect of manufacturing defects were studied [16] and the design improvements were extended to other frequency bands, such as 0.2–2, 18–40, 0.1–1 and 10–100 GHz [17–19].

A number of recent studies and developments have resulted in DRGH antenna designs with bandwidth ratios extending beyond 18:1 [20,21]. The original design presented in [20] had an operating bandwidth of 1–18 GHz, but according to the datasheet [21] the antenna can be used from 0.8 GHz for a bandwidth ratio of 22.5:1. A number of changes were made: the ridge profile was changed and the ridges extended beyond and over the *H*-plane sidewalls. For ease of manufacture cut-outs were made in the *H*-plane sidewalls for the ridges to pass through. This horn antenna had aperture dimensions of 30.5 cm × 28 cm. Carbon loaded foam absorber was placed in the back of the ridge cavity [20]. A design similar to that in [11,12] was presented in [22], with the cavity filled with a magnetic loaded silicone absorber (ECCOSORB FDS). The widest bandwidth DRGH design reported thus far, 0.6–50 GHz (83:1 bandwidth), was presented in [23], but a lack of information makes it difficult to validate the design and only selective simulation results were reported. The design is based on [13], but without the plane sidewalls. To achieve this

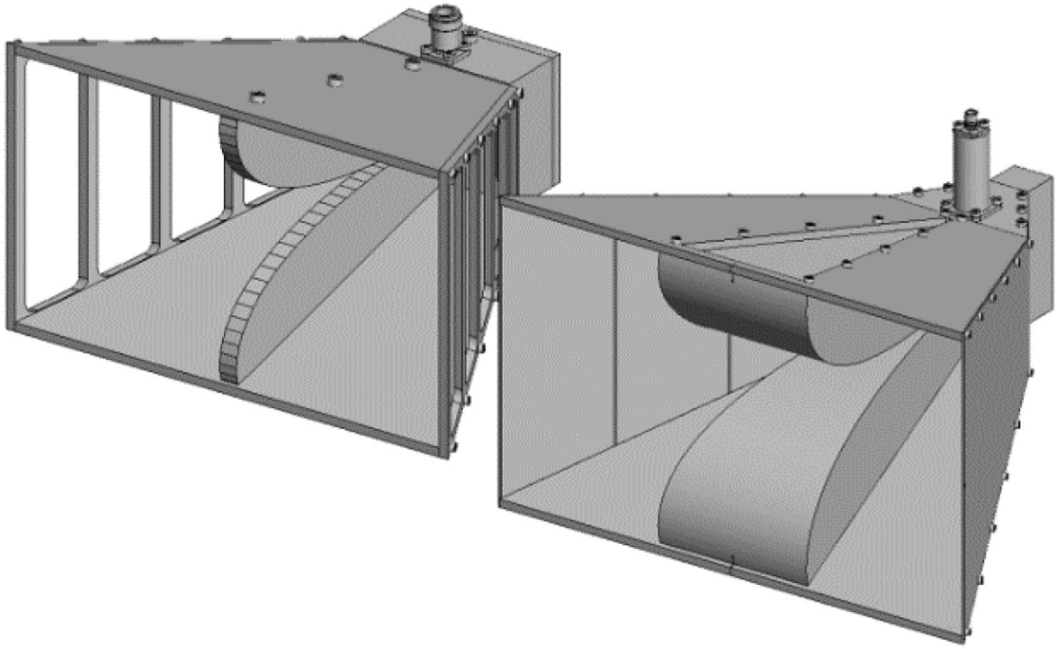

FIGURE 1 The conventional 1–18 GHz DRGH antenna (left) and the new 0.5–18 GHz DRGH antenna (right)

extended bandwidth, a Luneburg lens, perforations and absorber (ECCOSORB GDS) in the coaxial to waveguide launcher, were used.

Currently all the bandwidth extended designs (beyond 18:1) include either a dielectric lens or absorber or both, which restricts the use of these designs to lower power applications. A new 0.5–18 GHz (36:1) DRGH antenna design without a lens or absorber is proposed here. The wider bandwidth is achieved with a new cavity design and an optimised design combination of the other important antenna sections (coaxial feed, ridges, sidewalls and flared waveguide).

The new DRGH antenna is very compact, with aperture dimensions of 26.4 cm × 15.2 cm, which is less than 12% larger than the linear aperture dimensions (24.2 cm × 13.6 cm) of a conventional 1–18 GHz DRGH antenna.

Simulated and measured results for a prototype DRGH antenna are presented to validate the design. In Section 2, a detailed design of the new DRGH antenna is presented with measured and simulated results in Section 3. Section 4 contains a design analysis clarifying the impact of the various antenna subsections on the overall antenna performance. The 0.5–18 GHz DRGH antenna performance is compared to other commercially available DRGH antennas in Section 5, with concluding remarks in Section 6.

2 | DRGH ANTENNA DESIGN AND SIMULATIONS

Typical modern radar electronic support measures (RESM) systems and antennas cover the frequency ranges 0.5–18 and 18–40 GHz. In most cases, the 0.5–18 GHz band is split into multiple bands, but there are some antennas/systems that cover the whole band with a single unit [24]. The purpose of this research is to design an antenna that can be used to measure 0.5–18 GHz antennas and systems in a single band, as a source antenna in an anechoic chamber, a gain reference antenna, and for EMC/I testing. As the largest antenna to be measured is 200–300 mm in diameter, the horn antenna aperture cannot be significantly larger if it is to be used as an accurate gain reference. The antenna should be able to transmit moderate to high power, which precludes the use of absorber. A voltage standing-wave ratio (VSWR) of below 2:1 is required with maximum peaks below 2.5:1. A new 0.5–18 GHz DRGH antenna that meets these requirements was designed as an improvement on the 1–18 GHz design presented in [13]. Both antennas are shown in Figure 1. The design of each of the different sections of the new DRGH antenna is discussed in more detail below.

2.1 | Design of the coax to ridged waveguide launcher

The coax to ridged waveguide launcher is one of the most crucial parts of the horn antenna design. The launcher must ensure that the unbalanced coaxial feed is transformed to a balanced double-ridged waveguide geometry, effectively performing the role of a balun, while suppressing higher order modes that could cause pattern deterioration. Various geometries have been used in the past as illustrated in Figure 2. The first designs used a basic empty box cavity (Figure 2, top left) [2,7,25–28]. In most empty box cavities, the ridge is stepped down and extended into the cavity up to the back short. This design can typically operates over bandwidths of 3:1 to 9:1.

The most common, traditional design uses a box cavity filled with *E*-plane flares and *H*-plane wedges (Figure 2, top

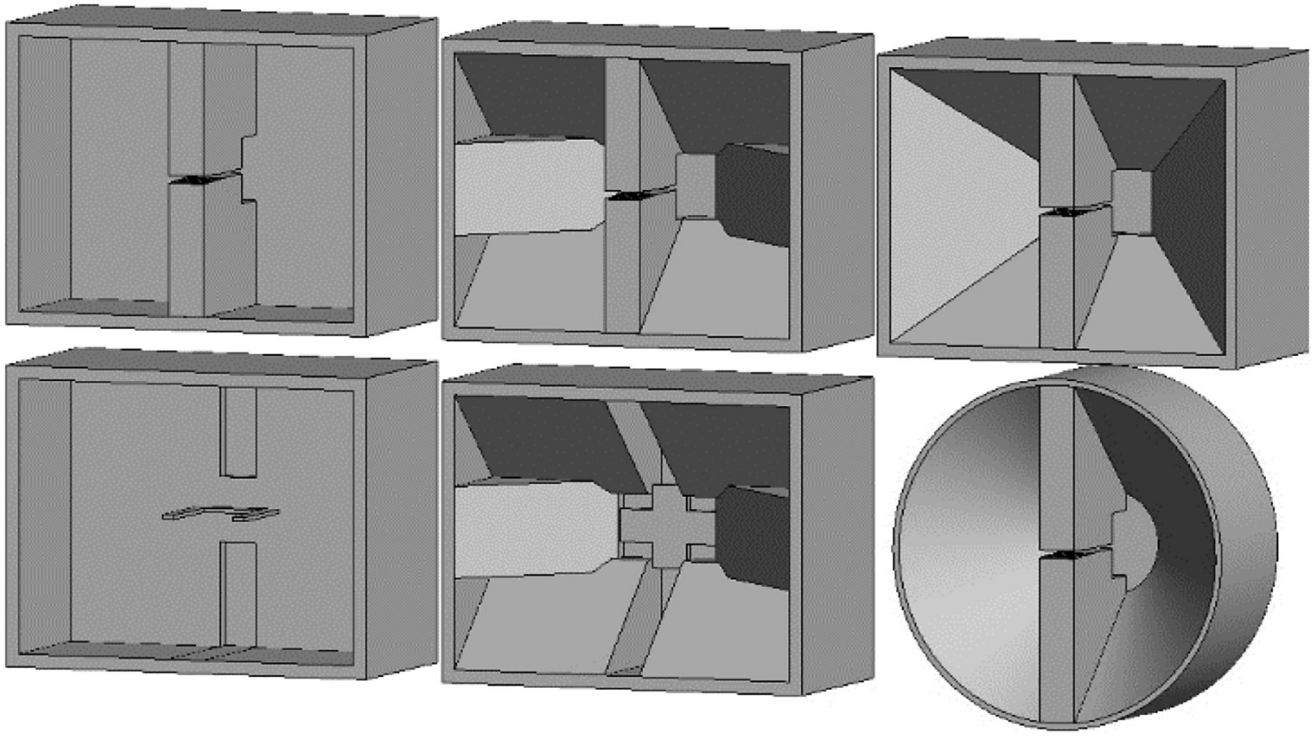

FIGURE 2 Previous coax to waveguide launcher designs

FIGURE 3 Different cavity shapes considered during the parametric study of the coax to waveguide launcher (the ridges are omitted for clarity)

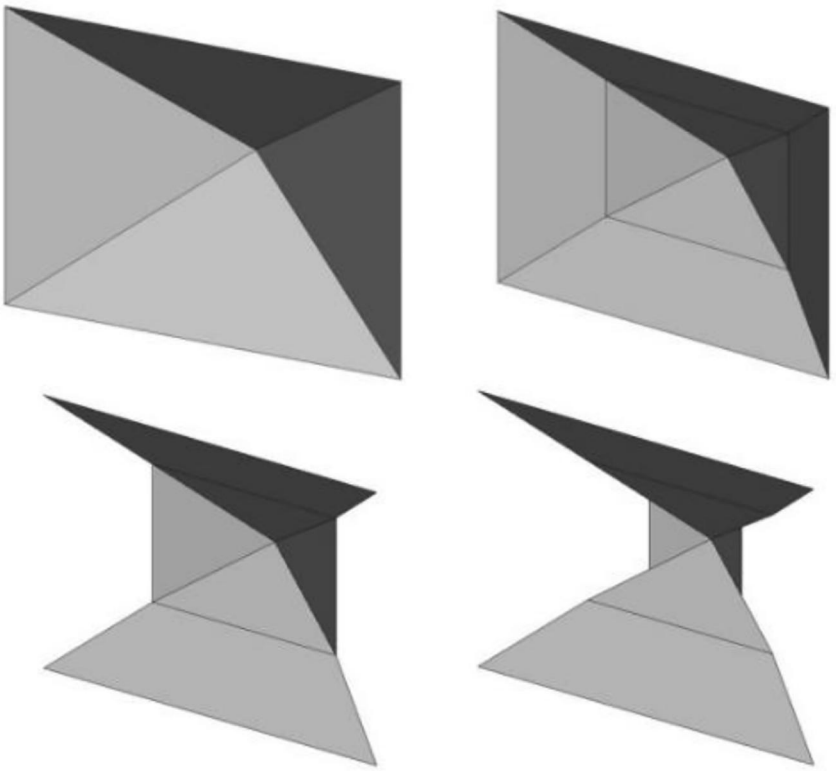

centre) [8,9,14–17,22,29]. The ridge is also stepped down and extended into the cavity; which, along with the back short, forms a smaller rectangular box cavity.

These two designs cannot suppress unwanted modes in wideband designs with bandwidths in excess of 12:1, usually resulting in pattern deterioration above 12 GHz. The

introduction of mode suppressing fins is a variation of the basic box design (Figure 2, bottom left, with the ridges omitted for clarity). This resulted in designs without pattern deterioration over bandwidths of 18:1 [11,12,29]. The inclusion of a cross-shaped structure in the small rectangular box cavity is a variation of the traditional flare and wedge design (Figure 2, bottom centre, with the ridges omitted for clarity) [30]. This design resulted in an 18:1 bandwidth without pattern deterioration.

Pyramidal and semi-pyramidal cavities also evolved from of the traditional flare and wedge design (Figure 2, top right) [13,23,31,32]. These designs also allow wideband operation without pattern deterioration. Another advantage of the pyramidal cavity is ease of manufacture since the entire launcher can be manufactured from a single part. A conical launcher (Figure 2, bottom right) is discussed in [33].

Although numerous designs of the launcher have been proposed, none of these geometries allow operation over significantly wider bandwidths than 18:1 without the use of absorbing materials. The coax to ridged waveguide launcher is therefore redesigned to achieve the following goals:

- to extend bandwidth of operation from 0.5 to18 GHz (36:1),
- to ensure no pattern deterioration at higher frequencies, and
- to use the minimum number of subsections for ease of manufacturing.

The waveguide launcher of [13] was redesigned after a structured parametric study for different cavity shapes (Figure 3). The launcher configuration was changed, step by step, from a pyramidal cavity (Figure 3, top left) to a multi-step open cavity (Figure 3, bottom right). A full parametric study was performed for each configuration. A two-port model was used to accelerate the simulation process of the coax to ridged waveguide launcher. The method of moments (MoM) was primarily used, with a coaxial waveguide port. Due to the requirements imposed by the numerical tool (FEKO), the double-ridged waveguide was terminated in a thin (1 mm thick) air-filled finite element method (FEM) region with a FEM modal port. The final configuration of the launcher is shown in Figure 3 (bottom right). The simulated reflection coefficient of the launcher is compared to that of the complete horn antenna in Figure 4. The geometries of the initial waveguide launcher [13] and the newly designed launcher are shown in Figure 5. The block at the rear of the waveguide launcher in Figure 5 (right) is only used for mounting purposes, for example, in an anechoic chamber. The final configuration can be described as a partially open boundary, multi-stepped flared and pyramidal waveguide launcher.

A step was inserted right at the feed point, reducing the ridge gap in that area to 0.7 mm, to improve the high frequency performance and prevent pattern deterioration at 18 GHz. The maximum usable bandwidth increases very rapidly as the gap between the ridges is reduced [2]. To allow performance up to 18 GHz without pattern deterioration, the ridge gap must be approximately 1 mm or less.

The transverse resonance method [3,4,34] can be used to design ridged waveguides. The cut-off wavelengths, λ_c, for the TE_{no} modes can be determined from [2]:

$$\frac{B}{D}tan\theta_2 - cot\theta_1 + \frac{B_c}{Y_{01}} = 0 \quad (1)$$

$$\frac{B}{D}cot\theta_2 + cot\theta_1 - \frac{B_c}{Y_{01}} = 0 \quad (2)$$

where

$$\theta_1 = \frac{\pi(A-S)}{\lambda_c} = \pi\left(1-\frac{S}{A}\right)\left(\frac{A}{\lambda_c}\right) \quad (3)$$

$$\theta_2 = \frac{\pi S}{\lambda_c} = \pi\left(\frac{S}{A}\right)\left(\frac{A}{\lambda_c}\right) \quad (4)$$

with A, B, S and D the cross-sectional dimensions of the ridged waveguide as defined in Figure 6. Equation (1) is applicable to the TE_{no} modes when n is odd and Equation (2) when n is even, with the discontinuity susceptance, $\frac{B_c}{Y_{01}}$ for double ridged waveguide [34]:

$$\frac{B_c}{Y_{01}} = \frac{B}{\lambda_c}\left[\frac{\alpha^2+1}{\alpha}cosh^{-1}\left(\frac{1+\alpha^2}{1-\alpha^2}\right) - 2ln\left(\frac{4\alpha}{1-\alpha^2}\right)\right] \quad (5)$$

$$\alpha = \frac{D}{B} \quad (6)$$

The cut-off frequency for the TE_{10} mode, using the dimensions in Figure 6, is 421 MHz. With the feed pin/probe in the centre of the ridge, the next expected higher order mode is TE_{30} [2]. The cut-off frequency for the TE_{30} mode is 4.36 GHz for a maximum usable bandwidth $\frac{\lambda_c^{10}}{\lambda_c^{30}}$ of 10.4:1, which is significantly smaller than what was achieved.

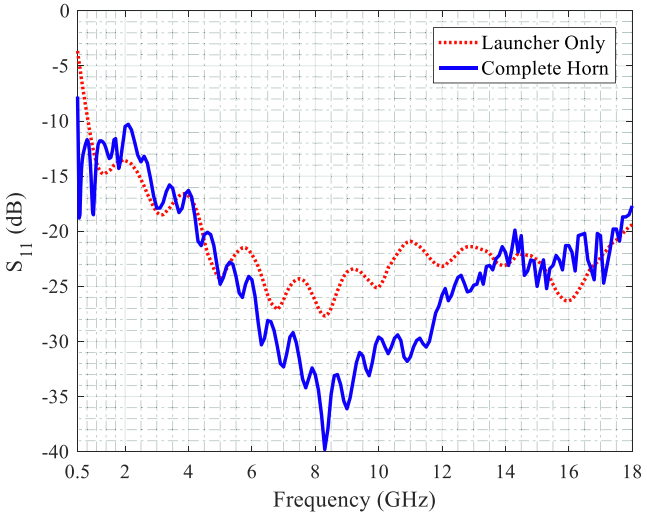

FIGURE 4 Reflection coefficient of the launcher section only and the complete DRGH

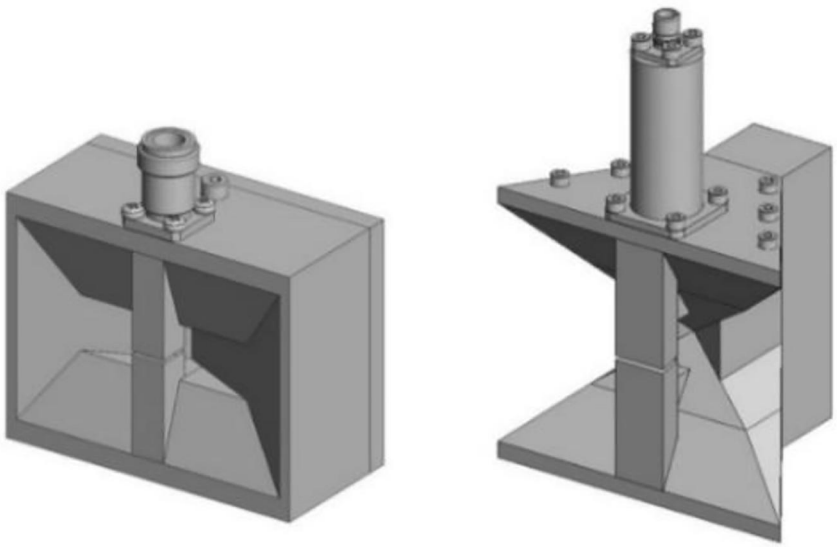

FIGURE 5 Comparison of the existing 1–18 GHz DRGH antenna waveguide launcher (left) and the new 0.5–18 GHz DRGH antenna launcher (right)

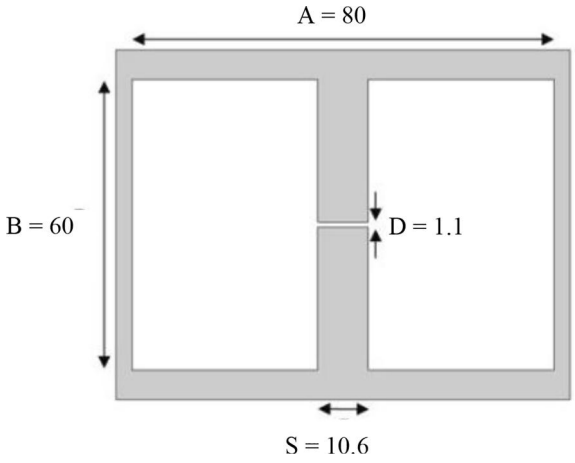

FIGURE 6 Ridged waveguide cross section definitions and final dimensions (mm) at launcher to flared waveguide section interface

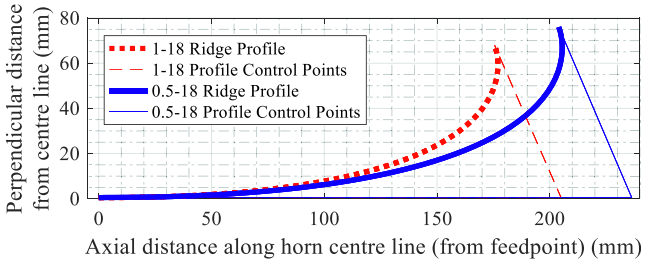

FIGURE 7 Comparison of the ridge profiles of the existing 1–18 GHz and the new 0.5–18 GHz DRGH antennas

2.2 | Design of the ridges

The ridge was redesigned using the approach followed in [35] except that a cubic Bezier ridge profile was used instead of an elliptical profile. The Bezier curve has better low frequency VSWR performance than the elliptical profile [36] and it can be modified to provide a better aperture match. A parametric study was performed to find the control points that provide the best VSWR.

The characteristic impedance for the TE_{10} mode in ridged waveguides at infinite frequency, $Z_{0\infty}$ is given by [2]:

$$Z_{0\infty} = \frac{1}{Y_{0\infty}} \tag{7}$$

where

$$\begin{aligned} Y_{0\infty} = 2\sqrt{\frac{\varepsilon}{\mu_0}}\,\frac{\lambda_c}{2\pi D}\Bigg\{ & \frac{2D}{\lambda_c}\cos^2\left(\frac{\pi S}{\lambda_c}\right)\ln\csc\left(\frac{\pi D}{2B}\right) \\ & + \frac{\pi S}{2\lambda_c} + \frac{1}{4}\sin\left(\frac{2\pi S}{\lambda_c}\right) \\ & + \frac{D}{B}\frac{\cos^2\left(\frac{\pi S}{\lambda_c}\right)}{\sin^2\left(\frac{\pi}{\lambda_c}(A-S)\right)}\left[\frac{\pi(A-S)}{2\lambda_c}\right. \\ & \left. - \frac{1}{4}\sin\left(\frac{2\pi(A-S)}{\lambda_c}\right)\right]\Bigg\} \end{aligned} \tag{8}$$

$$Z_0 = Z_{0\infty}\Big/\sqrt{1-(f_c/f)^2} \tag{9}$$

At the launcher-waveguide interface, $Z_{0\infty}$ was calculated using the dimensions in Figure 6 as $Z_{0\infty} = 31\ \Omega$. The ridge profile transforms the wave impedance at the start of the flared waveguide to that of free space (377 Ω) at the horn aperture [2]. The ridge width was tapered linearly from 10.6 mm at the start of the flared section to 84.4 mm at the aperture. The final

TABLE 1 Cubic Bezier control points of the final ridge profile of the new 0.5–18 GHz DRGH antenna (in mm)

Bezier point	Description	Axial distance (X)	Perpendicular distance (Y)
P0	Start point	3.3	0.55
P1	Start tangent point	236.32	0.55
P3	End tangent point	203.99	75.99
P4	End point	204	76

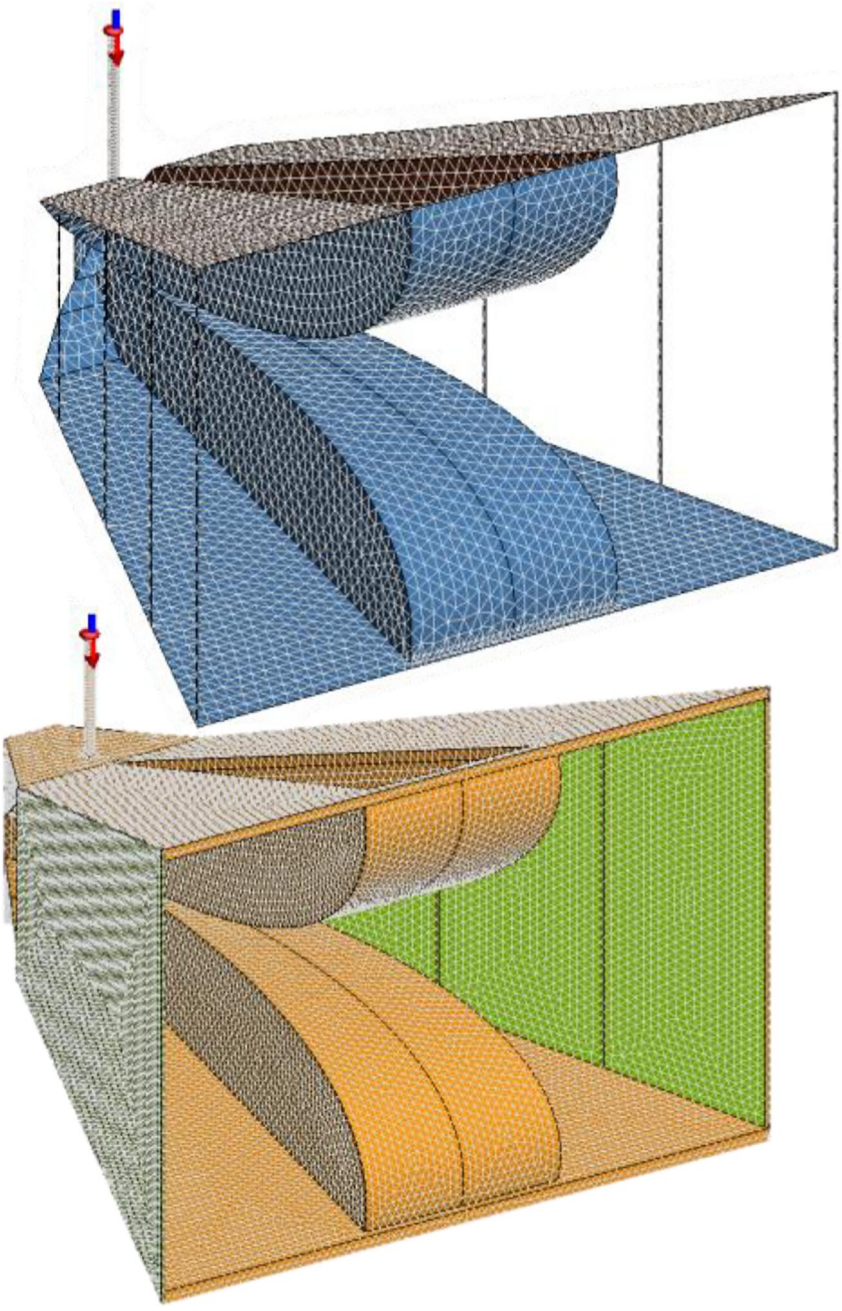

FIGURE 8 Simplified (top) and detailed (bottom) FEKO simulation model

ridge profile is shown in Figure 7 and the Bezier control points are given in Table 1.

Calculating the wave impedance at the aperture is not straightforward since the ridge is terminated slightly before the aperture and curves back slightly from its maximum axial length (Figure 7). At a distance of 1.6 mm before the aperture the wave impedance is close to free space; $Z_{0\infty} = 376\ \Omega$. A constant ridge width in a short axial length broadband horn antenna causes an undesirable peaked amplitude distribution in the *H*-plane and large phase error in the *E*-plane, resulting in reduced gain [2].

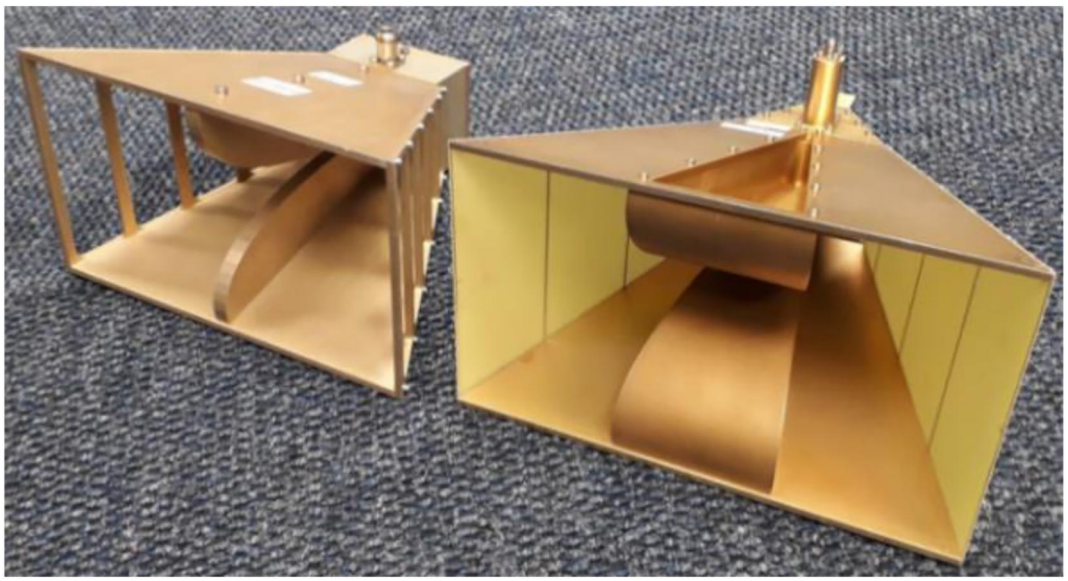

FIGURE 9 Photograph of the 1–18 GHz DRGH antenna (left) and the 0.5–18 GHz DRGH antenna (right)

Increasing the width of the ridges inside the flared section improves the gain as well as the bandwidth of the antenna.

2.3 | Design of the coaxial feed

The design of the coaxial feed is similar to that presented in [13], that is, with the outer conductor a hole through the upper ridge and the centre conductor a pin inserted into the connector terminating on the bottom ridge. The diameter of the hole cut through the top ridge forming the shield of the air-filled coaxial transition was kept constant at 3.7 mm. The coaxial feed was used as an impedance taper with the feed pin size increasing from 1.6 mm at the connector (50 Ω) to 2.2 mm on the bottom ridge (31 Ω). The diameter of the feed pin was linearly tapered for ease of manufacture. Ideally the transition length should be $\lambda/2$ at the lowest frequency of operation, but to avoid extension beyond the horn aperture the transition length was restricted to 75 mm ($\lambda/2$ at 2 GHz). Extending the transition further or implementing a different taper (e.g., a Hecken taper) might improve the low frequency VSWR performance.

The bottom ridge was machined so that spring fingers extracted from an N-Type connector could be inserted into the ridge in order to capture the feed pin with good electrical contact. This part of the transition and the exact location of the spring fingers were found to be extremely sensitive resulting in a large variation of the high frequency gain and VSWR performance of the DRGH antenna. Silver epoxy was applied around the spring fingers to remove any air gaps.

2.4 | Design of the flared waveguide section

The flared waveguide section is slightly larger than the design presented in [13]. The aperture width is 264 mm and the aperture height is 152 mm. The horn axial length from the launcher aperture to the horn aperture is 185 mm. The flared waveguide section was designed with solid *H*-plane sides, and a 0.8 mm FR4 substrate with etched grids was used for the *E*-plane sides. The strip width is 1 mm and the gap between strips $\lambda/10$ at 0.5 GHz (60 mm) to simulate a plane reflector at the low end of the band. It was found that wider strips or solid large rods had a detrimental effect on the low band VSWR. At higher frequencies where the spacing becomes more than half a wavelength, the gridded sidewall has a negligible effect [7].

2.5 | The FEKO simulation model

Two numerical electromagnetic (EM) models were developed in FEKO [37] using MoM to simulate the complete horn. The first model shown in Figure 8 (top) included numerous simplifications, for example, the exclusion of a connector and the dielectric material of the *E*-plane sidewalls, as well as the use of infinitely thin plates. This model was used for the design and optimisation of the complete horn in a reasonable amount of time. The final simulation was performed using the model, Figure 8 (bottom), before the prototype was manufactured. This model included more detail such as the dielectric support material, metal thickness and a model for the SubMiniature version A (SMA) connector.

Magnetic symmetry in the *E*-plane reduces runtime and required memory for both these models. Both models used perfectly conducting metallic (PEC) triangles to model the conductors and the detailed model used the surface equivalence principle (SEP) to model the dielectric supports and connector core. The general triangle edge length was $\lambda/5$ at 18 GHz for the detailed model and $\lambda/3$ (the minimum allowed in FEKO) for the simplified model. Smaller local mesh sizes were used in sensitive regions, for example around the ridge gap and

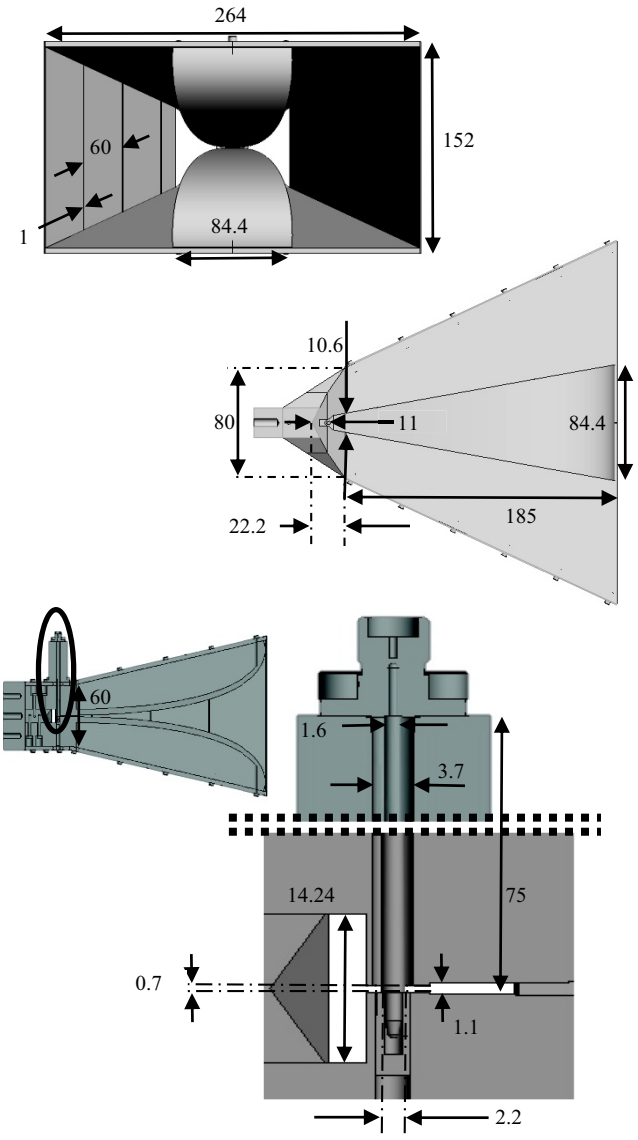

FIGURE 10 Final dimensions (in mm) of new 0.5–18 GHz DRGH antenna

feed as well as to get a more accurate representation of the geometry at locations with small features like the coaxial feed and feed pin. The general triangle edge lengths in those areas were set between λ/10 and λ/20. This resulted in 7190 PEC triangles for the simplified model and the detailed model consisted of 25870 PEC triangles and 6577 dielectric triangles.

Simulations were performed at 201 frequency points between 0.5 and 18 GHz. The frequency step size was 25 MHz below 1 GHz, 50 MHz between 1 and 2 GHz and 100 MHz above 2 GHz. All the simulations were performed using 12 parallel cores on one central processing unit (CPU). For the simplified model, the per core peak memory requirement was 153–170 MB (total peak of 1.8 GB) and the per core runtime 4.7 h (total of 56.4 h). For the detailed model, the per core peak memory requirement was 4.4–4.5 GB (total peak of 52.5 GB) and the per core runtime 201 h (total of 2411 h).

TABLE 2 Final dimensions of new 0.5–18 GHz DRGH

Description	Dimension (mm)
H-plane launcher width	80
E-plane launcher width	60
H-plane aperture width	264
E-plane aperture width	152
Ridge width (launcher interface)	10.6
Ridge width (aperture)	84.4
Ridge gap (at feed point)	0.7
Ridge gap (launcher interface)	1.1
Feed point to back wall	11
Launcher aperture to back wall	22.2
Ridge cavity step	14.24
Flared waveguide axial length	185
Feed pin diameter (start)	1.6
Feed pin diameter (stop)	2.2
Feed pin length	75
Feed outer conductor diameter	3.7
Sidewall strip width	1
Sidewall grid gap	60

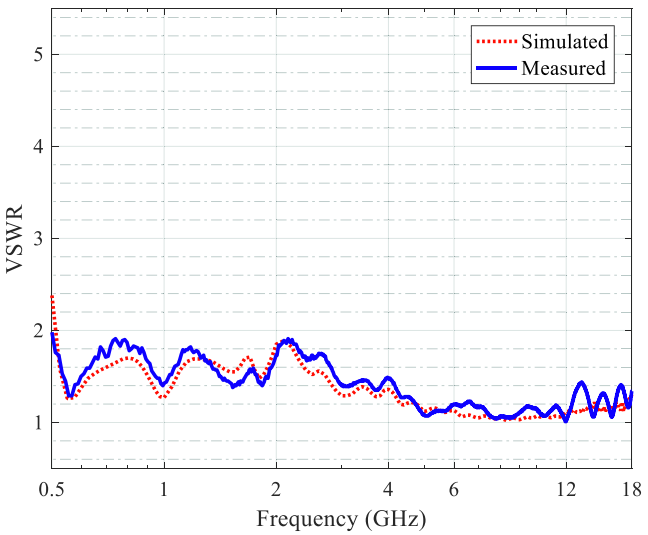

FIGURE 11 Simulated and measured VSWR

2.6 | Prototype manufacturing

Based on the final FEKO model a prototype was manufactured (Figure 9). The parts were machined from aluminium except for the feed pin that was manufactured from brass and then gold-plated. The prototype used an SMA connector for ease of assembling and testing, but can easily be redesigned to use an N-type connector for high power applications. Care was taken to use the minimum number of components to reduce the

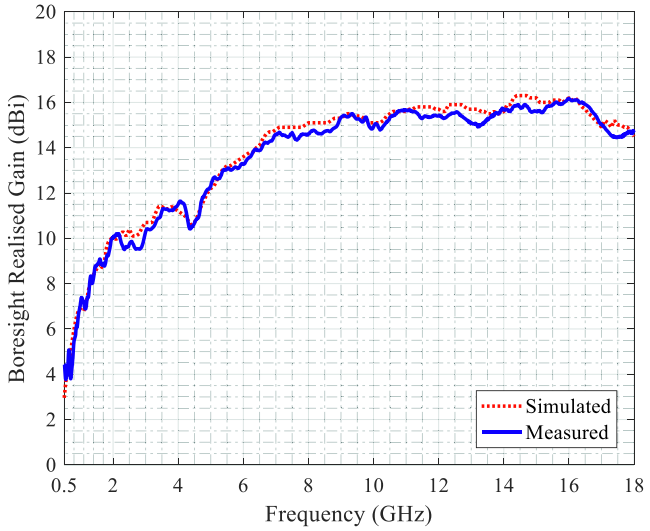

FIGURE 12 Simulated and measured realised gain on boresight

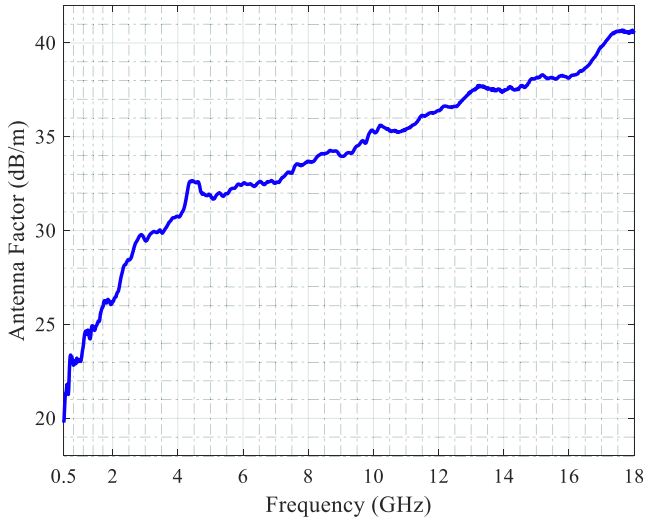

FIGURE 13 Measured antenna factor

possibility of gaps between the subsections [16]. A special effort was made to reduce the weight of the antenna, particularly the ridges. The final weight is 1.78 kg. The final dimensions (all in mm) are presented in Figure 10 and summarised in Table 2.

3 | SIMULATED AND MEASURED RESULTS

The measured and simulated VSWR are compared in Figure 11. In previous studies, a linear frequency scale was used for VSWR; however, due to the extreme bandwidth this makes it difficult to observe the ripple structure at the lower frequencies, therefore a logarithmic frequency scale is used. The agreement between measured and simulated results is very good. The ripple above 12 GHz is due to manufacturing tolerances and a very sensitive feed region. The VSWR is below 2:1 over the whole band and below 1.5:1 above 3 GHz.

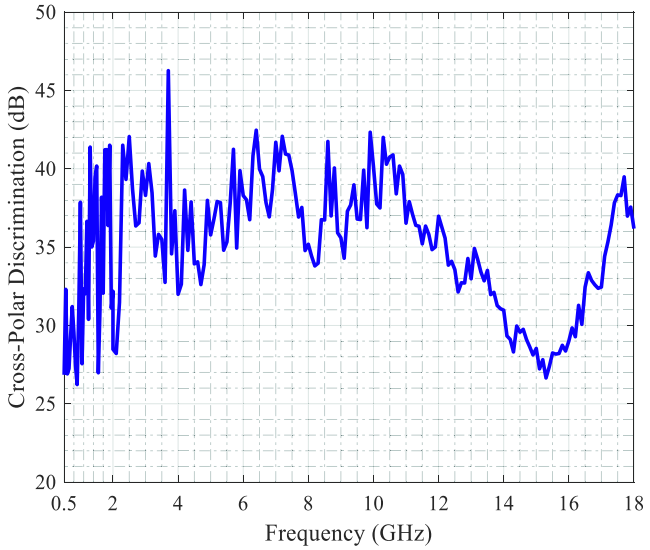

FIGURE 14 Minimum cross-polar discrimination within ±10° from boresight

The gain and pattern measurements were performed in a tapered anechoic chamber with two different setups namely the low band 0.5–2 GHz and the high band 2–18 GHz. For the low band setup, gain was measured in 10 MHz steps and patterns in 50 MHz steps; the high band gain was measured in 25 MHz steps and patterns in 100 MHz steps. Radiation patterns were measured for the *E*-, *H*-, and 45°-planes, co- and cross-polarisation. All patterns were measured from 0 to 360° in 2° increments.

A comparison of the measured and simulated boresight realised gain is shown in Figure 12. The gain changes rapidly between 0.5 and 2 GHz. A linear scale is used to allow easy comparison with previous results. The measured and simulated results are typically within the measurement accuracy of ±0.5 dB. The minimum gain at 0.5 GHz is approximately 4 dBi and increases to approximately 16 dBi at 16 GHz. The small differences in measured and simulated realised gain can be attributed to the difference in simulated and measured VSWR.

The measured antenna factor in Figure 13 increases from around 20 dB/m at 0.5 GHz to 41 dB/m at 18 GHz at a rate of between 2 and 5 dB per octave.

The cross-polar discrimination is an important parameter to observe. A low cross-polar discrimination at the high frequency end is indicative of pattern breakup [13], whereas a source antenna with high cross-polar discrimination is required to accurately measure circularly polarised antennas in an anechoic chamber. The measured minimum cross-polar discrimination within ±10° from boresight is shown in Figure 14 and is typically better than 30 dB except below 2 GHz and around 15 GHz where it decreases to 26 dB.

The measured co-polarised radiation patterns for the *E*-, *H*-, and 45°-planes at discrete frequencies are presented in Figure 15. It is evident that this antenna does not have pattern breakup at the high frequency end of the band.

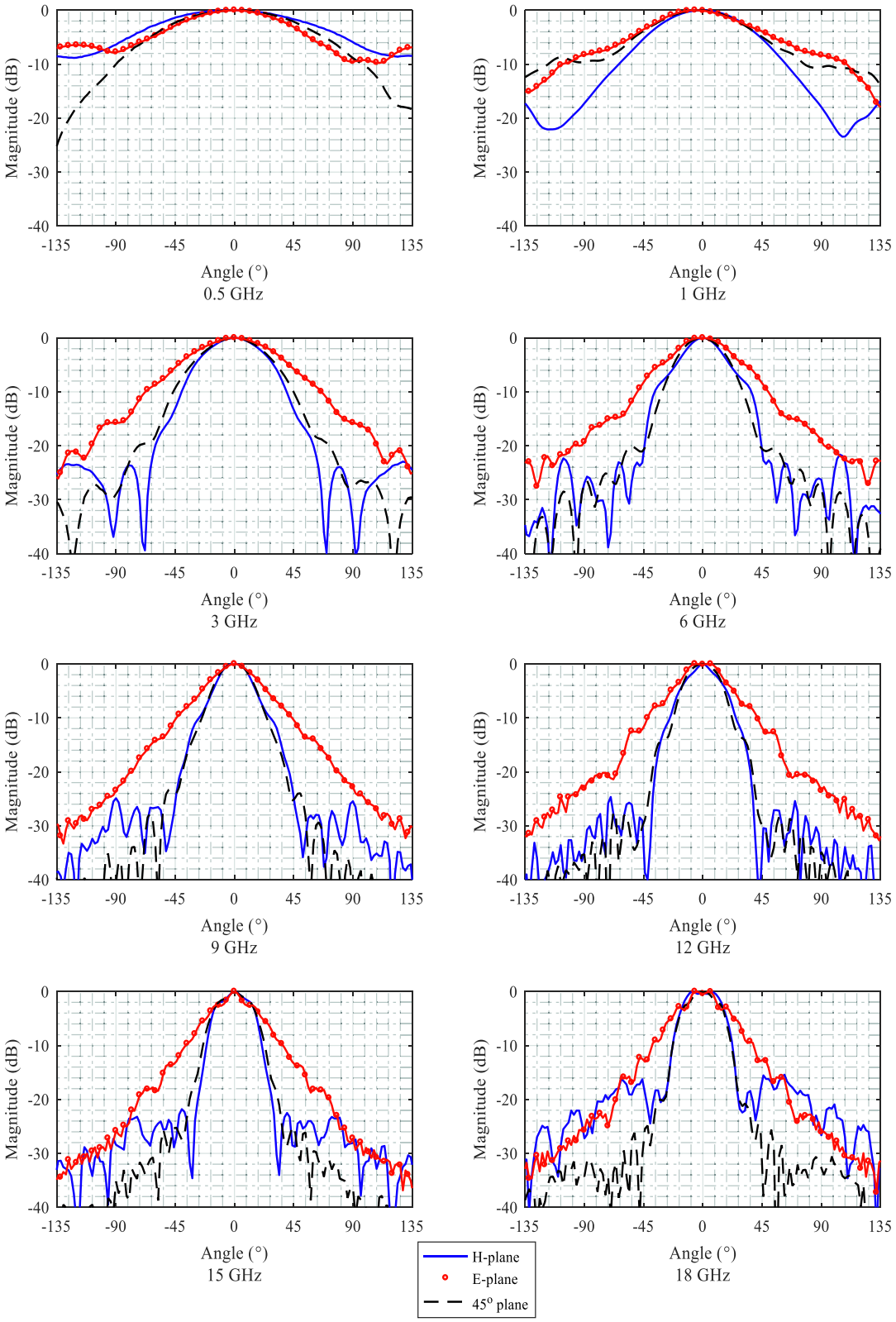

FIGURE 15 Measured co-polarised radiation patterns of the 0.5–18 GHz DRGH antenna

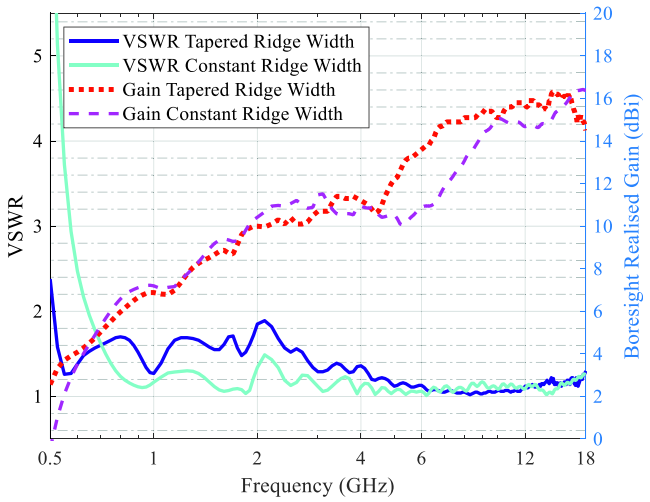

FIGURE 16 Simulated VSWR and boresight gain with tapered and constant ridge widths

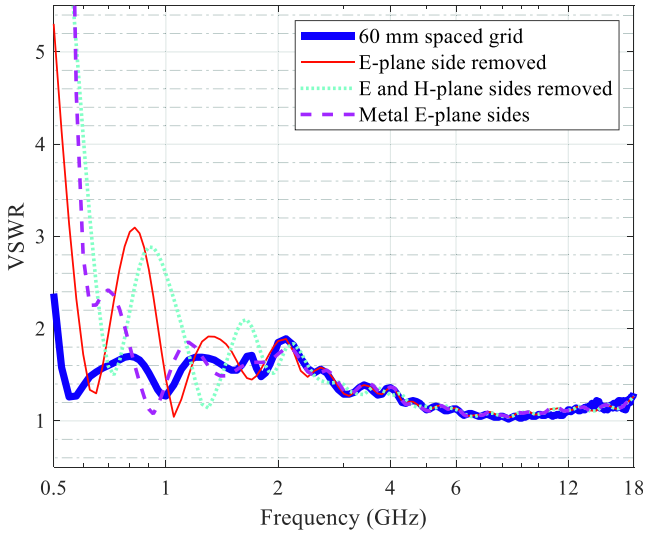

FIGURE 17 Simulated VSWR with different sidewalls

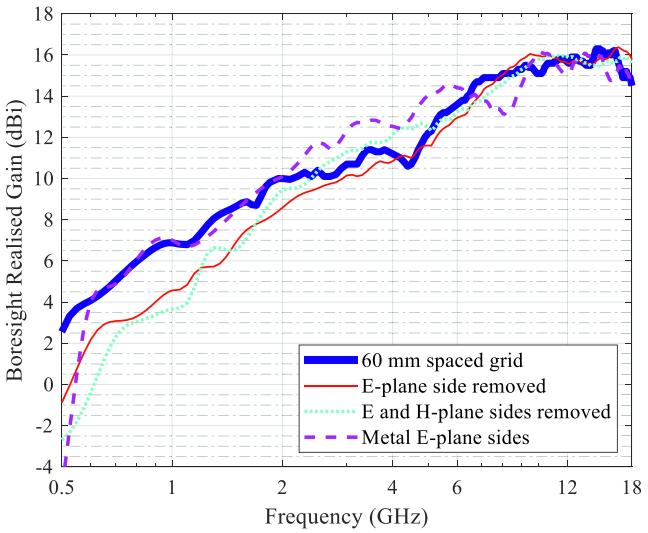

FIGURE 18 Simulated boresight gain with different sidewalls

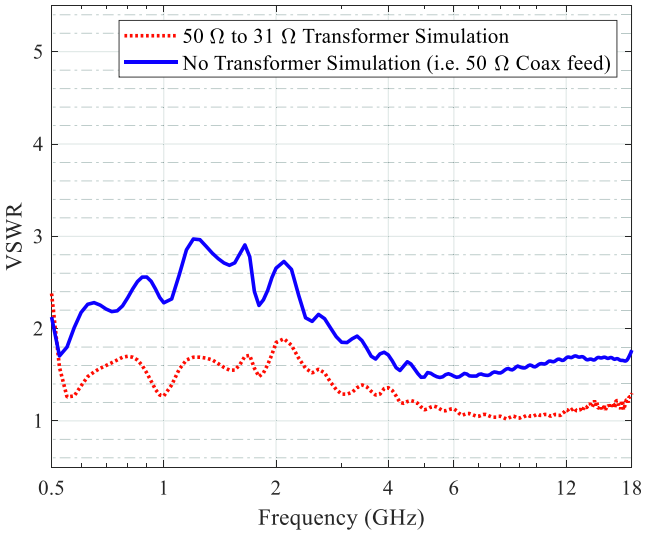

FIGURE 19 VSWR improvement due to coaxial impedance transformer

4 | DESIGN ANALYSIS

This section focuses on the impact of several of the most important design aspects.

4.1 | Impact of the ridge width

Apart from providing improved gain as shown in [35], it was also found that the tapered ridge width improves the bandwidth. Figure 16 compares the VSWR of the tapered and a constant ridge width, with the VSWR above 2.5:1 below 0.6 GHz for the constant ridge width. The boresight gain comparison also in Figure 16 shows the improved gain of the tapered ridge width above 4 GHz and below 0.6 GHz.

4.2 | Impact of the sidewalls

The sidewalls have a significant effect on the low frequency performance, but very little effect at higher frequencies. Figure 17 shows the VSWR comparison when the *E*-plane and both *E*- and *H*-plane sidewalls are removed, as well as when the *E*-plane sidewalls are replaced by metal sidewalls. The bandwidth is reduced and the VSWR peaks dramatically increase in magnitude below 2 GHz.

Since the effect of the sidewalls is only visible below 4 GHz, the boresight gain is plotted (Figure 18) using a logarithmic frequency scale. At the low frequency end the gain drops significantly when removing the sidewalls, but at the high frequencies (above 4 GHz) removal of the sidewalls has very little effect. This is because the fields at high frequencies are concentrated between the ridges and the

TABLE 3 CST mode information

Mode number	Type	f_c (GHz)	Mode number	Type	f_c (GHz)
1	TE	0.13	14	TM	13.21
2	TE	4.36	15	TE	13.89
3	TE	5.03	16	TM	13.89
4	TE	6.65	17	TE	14.99
5	TM	6.6	18	TE	15.59
6	TE	8.65	19	TM	15.6
7	TE	9.99	20	TE	16.3
8	TM	9.98	21	TM	16.37
9	TE	10	22	TE	17.26
10	TM	10.89	23	TE	17.29
11	TE	10.9	24	TM	17.3
12	TE	12.97	25	TE	17.96
13	TE	13.21			

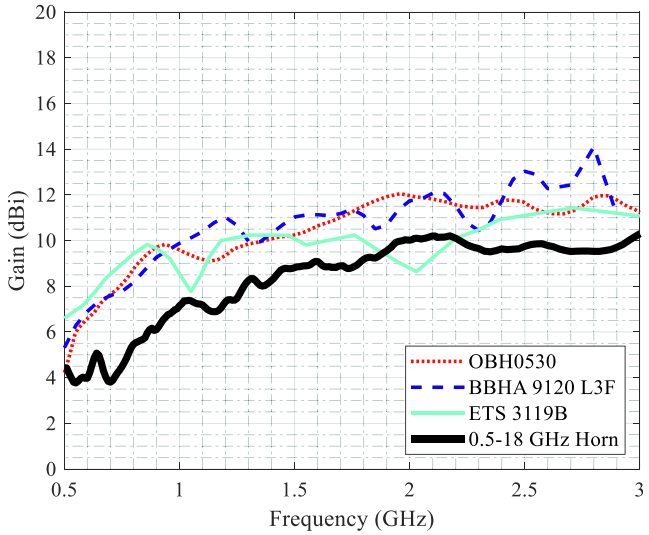

FIGURE 20 Gain performance comparison low band

antenna operates more like a three-dimensional traveling wave Vivaldi or TEM horn antenna than a flared waveguide horn antenna.

4.3 | Impact of the tapered impedance transformer

Using the coaxial feed as an impedance transformer from the 50 Ω impedance of the connector to the lower impedance of the ridged waveguide (31 Ω) has a significant effect. The comparison of the VSWR for the antenna with and without the impedance transformation (Figure 19) shows that the impedance transformer significantly improves the VSWR performance across the whole band except right at 0.5 GHz.

4.4 | Modal field and bandwidth analysis

In Section 2.1 it was shown that the expected maximum usable bandwidth $\frac{\lambda_c^{10}}{\lambda_c^{30}}$ as calculated using the transverse resonance method is only 10.4:1. A thorough parametric study in simulation ultimately resulted in a design with 36:1 bandwidth.

A modal study performed in CST [38] for a double-ridged waveguide with dimensions given in Figure 6, showed that at least 25 modes can propagate in the 0.5–18 GHz frequency band. The modes that can possibly propagate and their corresponding cut-off frequencies are listed in Table 3. It is clear from the performance of the proposed antenna over the full 36:1 bandwidth that although the double-ridged waveguide supports high order modes, these modes are either not excited or the coupling from the coaxial feed to the higher order modes is so small that they do not impact the input impedance or radiation patterns of the DRGH.

5 | Comparison to commercially available antennas

The increased operational bandwidth of the proposed antenna now makes it possible for a single antenna to cover the full frequency range 0.5–18 GHz, as opposed to at least two antennas in the past. Even though the production cost for the proposed horn may be around 30–40% higher than a conventional 1-18 GHz DRGH antenna, due to the complexity of the ridges and the larger size of the antenna, requiring only one horn will be much more cost-effective.

Figure 20 compares the boresight gain of the 0.5–18 GHz antenna to three commercially available DRGH antennas in the low band (0.5–3 GHz): OBH0530 from Ocean Microwave, BBHA 9120 L3F from Schwarzbeck and ETS 3119B from ETS-Lindgren. The antennas were chosen based on having the smallest size (aperture and axial length) available, while still working down to 0.5 GHz. The 0.5–18 GHz antenna has slightly less gain than the other antennas, but the gain in the low band is very stable and usable. Table 4 compares the dimensions of the four antennas, with the 0.5–18 GHz DRGH antenna approximately 40% smaller (linear aperture dimensions) and also significantly lighter than the other horns.

Figure 21 compares the boresight gain of the 0.5–18 GHz antenna to three commercially available DRGH antennas in the high band (0.7–18 GHz): DRH18-EX from RF Spin, BBHA 9120 D from Schwarzbeck and ETS 3115 from ETS-Lindgren. The new 0.5–18 GHz antenna has better and more constant gain across the band. Table 5 compares the dimensions of the antennas showing that the new 0.5–18 GHz horn dimensions are comparable to the other 0.7–18 GHz horns. The 0.5–18 GHz DRGH antenna therefore provides a very good size to performance trade-off with significantly better performance above 6 GHz and usable performance down to 0.5 GHz.

TABLE 4 Comparison of low band horn dimensions

Horn	Aperture dimensions (mm)	Axial length (mm)	Mass (kg)
OBH0530	440 x 290	350	6.8
BBHA 9120 L3F	416 x 243	342	3.8
ETS 3119B	488 x 314	400	5.2
0.5–18 GHz Horn	264 x 152	185	1.78

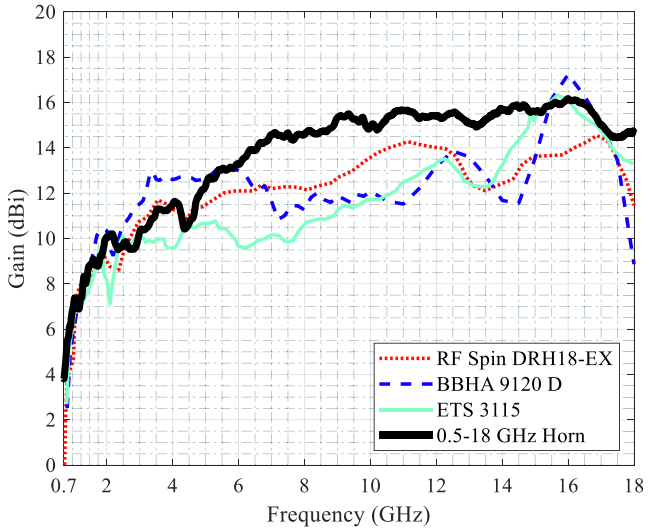

FIGURE 21 Gain performance comparison high band

TABLE 5 Comparison of high band horn dimensions

Horn	Aperture dimensions (mm)	Axial length (mm)	Mass (kg)
DRH18-EX	234 x 186	216	0.87
BBHA 9120 D	245 x 142	195	1.3
ETS 3115	244 x 159	279	1.8
0.5–18 GHz Horn	264 x 152	185	1.78

6 | CONCLUSION

A 0.5–18 GHz (36:1) DRGH antenna design was presented. The bandwidth was obtained using a new cavity design and ensuring that the design combination of the other important sections (coaxial feed, ridges, sidewalls and flared waveguide) allows wideband operation without using a lens or absorber. Simulated and measured results for a prototype DRGH antenna were presented to validate the design. The design is extremely compact with an aperture of 26.4 cm × 15.2 cm, less than 12% larger than the linear aperture dimensions of a conventional 1–18 GHz DRGH (24.2 cm × 13.6 cm), but with double bandwidth ratio.

ACKNOWLEDGEMENT

The authors would like to thank Saab Grintek Defence for the use of their anechoic chambers and production facilities.

ORCID

Bennie Jacobs https://orcid.org/0000-0002-0476-6041

REFERENCES

1. Radio Research Laboratory Harvard University: Very High Frequency Techniques, 725–728. McGraw-Hill, New York (1947)
2. Walton, K.L., Sundberg, V.C.: Broadband ridged horn design. Microw. J. 96–101 (1964)
3. Cohn, S.B.: Properties of ridge waveguide. Proc. IRE. 35(8), 783–788 (1947)
4. Hopfer, S.: The design of ridged waveguides. IRE Trans. Microw. Theory Tech. 3(5), 20–29 (1955)
5. Kerr, J.L.: A Very Broad Band Low Silhouette Antenna. Tech. Rep. ECOM-3087. USAECOM, Fort Monmouth(1967)
6. Kerr, J.L.: Broadband Horns. Tech. Rep. ECOM-3319. USAECOM, Fort Monmouth (1970)
7. Kerr, J.L.: Short axial length broad-band horns. IEEE Trans. Antennas Propag. 21(5), 710–714 (1973)
8. Bruns, C., Leuchtmann, P., Vahldieck, R.: Analysis and simulation of a 1–18 GHz broadband double-ridged horn antenna. IEEE Trans. Electromagn. Compat 45(1), 55–60 (2003)
9. Bruns, C., Leuchtmann, P., Vahldieck, R.: 'Comprehensive analysis and simulation of a 1–18 GHz broadband parabolic reflector horn antenna system'. IEEE Trans. Antennas Propag. 51(6), 1418–1422 (2003)
10. Bruns, C., Leuchtmann, P., Vahldieck, R.: Full wave analysis and experimental verification of a broad band ridged horn antenna system with parabolic reflector. In: IEEE Antennas and Propagation Society International Symposium. Boston (2001)
11. Rodriguez, V.: New Broadband EMC Double-ridged Guide Horn Antenna, 44–47.RF Design (2004)
12. Rodriguez, V.: Dual ridge horn antenna. US. Patent 6 995 728 B2 (2006)
13. Jacobs, B., Odendaal, J.W., Joubert, J.: An improved design for a 1–18 GHz double ridged guide horn antenna. IEEE Trans. Antennas Propag. 60(9), 4110–4118 (2012)
14. Botello-Perez, M., Jardon-Aguilar, H., Ruiz, I.G.: Design and simulation of a 1 to 14 GHz broadband electromagnetic compatibility DRGH antenna. In: Proceedings of 2nd international conference electrical and electronics engineering, 118–121. Mexico City (2005)
15. Abbas-Azimi, M., Arazm, F., Rashed-Mohassel, J.: Sensitivity analysis of a 1 to 18 GHz broadband DRGH antenna. In: IEEE Antennas and Propagation Society International Symposium, 3129–3132. Albuquerque (2006)
16. Jacobs, B., Odendaal, J.W., Joubert, J.: The effect of manufacturing and assembling tolerances on the performance of double-ridged horn antennas. J. Electromagnet. Wave. Appl. 24(10), 1279–1290 (2010)
17. Rodriguez, V.: Recent improvements to dual ridge waveguide horn antennas: The 200MHz to 2000MHz and 18GHz to 40GHz models. In: IEEE International Symposium on Electromagnetic Compatibility. Austin. 24–27 (2009)
18. Wei, L., XiaoLi, X.: Design and simulation of TEM double ridge guide horn antenna. In: Proceedings of 8th international conference on electronic measurement and instructions, 703–706.Xi'an (2007)
19. Morgan, M.A., Boyd, T.A.: A 10–100 GHz double-ridged horn antenna and Coax Launcher. IEEE Trans. Antennas Propag. 63(8), 3417–3422 (2015)
20. Steghafner, H., Leugner, D., Klos, B.: 'Horn Antenna'. U.S. Patent 7 969 376 B2 (2011)

21. Rohde & Schwarz, 'R&S HF907 Double-Ridged Waveguide Horn Antenna'. HF907 datasheet, HF – VHF/UHF Antennas, Catalog 2017/2018
22. Ghorbani, M.A., Khaleghi, A.: Double ridged horn antenna designs for wideband applications. In: 19th Iranian conference on electrical engineering, 1–4.ICEE, Tehran (2011)
23. Kuroptev, P.D., Levyakov, V.V., Fateev, A.V.: Modified 0.6–50 GHz ultra-wideband double-ridged horn antenna design for parameters improvement'. In: 2017 47th European microwave conference (EuMC), 465–468.Nuremberg (2017)
24. Randtron Antenna Systems, '6" C/J Band Spiral Antenna'. P/N 45460 datasheet (2014)
25. İsenlik, T., Başaran, E., Türetken, B.: A novel ultra wideband horn feed for parabolic reflector antennas. In: 2012 IEEE international conference on ultra-wideband, 513–517.Syracuse (2012)
26. İsenlik, T., Başaran, E., Türetken, B.: 'A novel 2–18 GHz double ridged horn antenna with an improved feed section design'. Electromagnetics. 35(3), 145–154 (2015)
27. İsenlik, T., Yegin, K., Barkana, D.E.: Near-constant beamwidth quadruple bandwidth double-ridged horn antenna design', IET Microwaves. Antenna. Propag. 12(12), 2102–2109 (2019)
28. Mallahzadeh, A.R.R., Dastranj, A.A., Hassani, H.R.: A novel dual-polarized double-ridged horn antenna for wideband applications. Progress Electromagnet. Res. B. 1, 67–80 (2008)
29. Abbas-Azimi, M., et al.: Design and optimization of a new 1–18 GHz double ridged guide horn antenna. J. Electromagnet. Wave. Appl. 21(4), 501–516 (2007)
30. Wang, C., et al.: Ridged horn antenna with adjustable metallic grid sidewalls and cross-shaped back cavity. IEEE Antenna. Wirel. Propag. Lett. 15, 1221–1225 (2016)
31. Xu, H., et al.: Design and simulation of ultra-wideband double-ridged horn antenna. In: International conference on microwave and millimeter wave technology, 950–952.Chengdu (2010)
32. Mallahzadeh, A.R., Imani, A.: Double-ridged antenna for wideband applications. Progress Electromagnet. Res. 91, 273–285 (2009)
33. Mallahzadeh, A.R., Dastranj, A.A.: Double-ridged conical horn antenna for 2–18 GHz. Electromagnetics. 28, 450–461 (2008)
34. Whinnery, J.R., Jamieson, H.W.: Equivalent circuits for discontinuities in transmission lines. Proc. IRE. 32, 98–116 (1944)
35. Gerber, M., Odendaal, J.W., Joubert, J.: DRGH antenna with improved gain and beamwidth performance. IEEE Trans. Antennas Propag. 68(5), 4060–4065 (2019)
36. Gerber, M., Odendaal, J.W., Joubert, J.: Ridge profile optimization of DRGH antenna. In: 2018 IEEE Radio and Antenna Days of the Indian Ocean (RADIO), 1–3.Grand Port (2018)
37. Altair, 'FEKO:Hyperworks: Release' (2019). https://altairhyperworks.com/ProductAltair.aspx?product_id=1019. Accessed August 2020
38. CST: CST Studio Suite 2020 Release. https://www.3ds.com/products-services/simulia/products/cst-studio-suite/. Accessed August 2020

How to cite this article: Jacobs B, Odendaal JW, Joubert J. Compact 0.5–18 GHz double-ridged guide horn antenna. *IET Microw. Antennas Propag.* 2021;15:427–440. https://doi.org/10.1049/mia2.12058